In situ evaluation of the initiation of the North Atlantic phytoplankton bloom

E. Boss[1] and M. Behrenfeld[2]

Received 1 June 2010; revised 30 June 2010; accepted 5 August 2010; published 21 September 2010.

[1] Two years of continuous physical and optical measurements from a profiling float in the western subarctic North Atlantic are used to analyze seasonal phytoplankton dynamics. The observed annual cycle challenges the traditional view that initiation of spring accumulations of phytoplankton in the upper water column requires a critical stratification threshold (known as the 'Gran effect' or the 'Sverdrup Hypothesis'). Instead, we find that biomass accumulation begins in mid-winter when light levels are minimal and near-surface mixing is deepest. These observations are consistent with the recently proposed dilution–recoupling hypothesis which states that deep winter mixing in the North Atlantic is essential for bloom formation as it decouples phytoplankton growth from grazing losses, thereby allowing net biomass accumulation despite low-light conditions.
Citation: Boss, E., and M. Behrenfeld (2010), In situ evaluation of the initiation of the North Atlantic phytoplankton bloom, *Geophys. Res. Lett.*, *37*, L18603, doi:10.1029/2010GL044174.

1. Introduction

[2] In many ocean regions, seasonal peaks in phytoplankton productivity result from coincident increases in intrinsic growth rates (i.e., carbon fixed per cell) and phytoplankton abundance (standing stock). The recurrent vernal (spring) phytoplankton bloom of the North Atlantic has been studied for nearly a century and is classically explained in most biological oceanography textbooks [*Miller*, 2004; *Mann and Lazier*, 2006] as a consequence of increased phytoplankton specific growth rates resulting from springtime mixed-layer shoaling and increasing light [*Sverdrup*, 1953; *Follows and Dutkiewicz*, 2002; *Siegel et al.*, 2002; *Henson et al.*, 2009]. Alternatively, some studies [*Evans and Parslow*, 1985] have espoused the view that biomass increases during blooms are primarily driven by alterations in predator–prey interactions (i.e., population loss terms), in addition to the light and nutrient factors responsible for increases in specific growth rates [*Banse*, 1994].

[3] In a recent study [*Behrenfeld*, 2010], satellite-based phytoplankton biomass data were employed to resolve annual cycles in net population growth rates and identify environmental conditions associated with initiation of the positive growth phase that leads to the spring biomass peak. Results from that study proved inconsistent with the classic light-driven interpretation of the North Atlantic bloom [*Sverdrup*, 1953] and instead suggested that phytoplankton biomass accumulation begins in early winter, prior to the onset of mixed layer shoaling. Based on these findings, *Behrenfeld* [2010] proposed a 'dilution–recoupling hypothesis' focused on a bio-physical explanation for bloom formation. According to this hypothesis, deep winter mixing acts to decouple phytoplankton growth and loss rates by diluting prey (phytoplankton) and predators (zooplankton), thereby relieving grazing pressure on the phytoplankton population by decreasing encounter rates between phytoplankon and grazers. Springtime restratification subsequently acts to simultaneously enhance phytoplankton specific growth rates and intensify predation loss rates, effectively 'recoupling' predators and prey when the phytoplankton and mobile grazers are again confined to a smaller water volume. The dilution–recoupling hypothesis thus allows for wintertime phytoplankton population growth rates comparable to those observed in spring, with biomass changes being largely independent of phytoplankton specific growth rates except under extreme low light conditions.

[4] A recent, multi-year deployment of an autonomous profiling float in the western North Atlantic has provided an opportunity to more thoroughly examine bloom initiation *in situ*. One source of uncertainty in *Behrenfeld*'s [2010] analysis stems from the limited detection depth of satellite ocean color measurements. Because remotely detected water-leaving radiances emanate from only the uppermost ocean layer, assumptions regarding the vertical structure of phytoplankton biomass within and below the photic zone were required for calculating population growth rates. In this paper, *in situ* vertical profiles of physical and optical data are used to examine annual cycles in phytoplankton biomass in a manner similar to that of *Behrenfeld* [2010], but with explicit characterization of vertical structure and deep phytoplankton entrainment during periods of mixed layer deepening. Consistent with the dilution–recoupling hypothesis, our *in situ* measurements indicate initiation of positive net population growth in mid-winter, rather than postponement until spring.

2. Methods

[5] In June 2004, a profiling float was deployed in the western North Atlantic carrying sensors to measure conductivity (C), temperature (T), pressure (Pr), particulate optical scattering, and chlorophyll fluorescence (Figure 1). Data presented in this paper were collected on 160 ascending profiles near local midnight every five days between June 2004 and September 2006, encompassing two winter seasons (the float then migrated south west across the N. Atlantic current). For each vertical profile, optical variables were despiked using a three-point-median filter. Chlorophyll

[1]School of Marine Sciences, University of Maine, Orono, Maine, USA.
[2]Department of Botany and Plant Pathology, Oregon State University, Corvallis, Oregon, USA.

0094-8276/10/2010GL044174

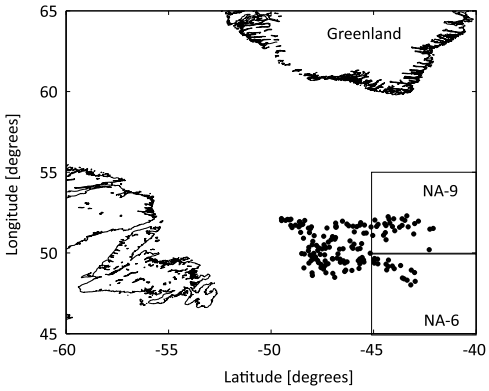

Figure 1. Float surfacing positions for the 160 profiles of the two-year dataset (black circles). Boxes *NA-9* and *NA-6* coincide with those defined in *Behrenfeld*'s [2010] SeaWiFS analysis of North Atlantic bloom development.

fluorescence was converted to chlorophyll concentration, [*chl*], as described by *Boss et al.* [2008]. Surface chlorophyll concentrations were calculated as the median of the upper four measurements of each profile (maximum depth 15 m), and these values were found to be in good agreement with satellite-derived (SeaWiFS) values of surface chlorophyll. Further details of the sampling protocols, data analyses, and uncertainty assessments are given by *Boss et al.* [2008].

[6] Phytoplankton carbon biomass (P) for each data point was estimated two ways; from particulate backscattering at 440 nm, $b_{bp}(440)$, and from chlorophyll concentration, [*chl*]:

$$P_b = \left(b_{bp}(440) - 0.00035 m^{-1}\right) \times 13000 \quad \left[m\mathrm{g\,m^{-3}}\right] \quad (1)$$

and

$$P_{chl} = [chl] \times 50 \quad \left[m\mathrm{g\,m^{-3}}\right]. \quad (2)$$

Equation (1) follows an approach developed for global estimations of P_b from satellite retrievals of b_{bp} [*Behrenfeld et al.*, 2005]. The quantity 13,000 mg C m^{-2} is a conversion factor formulated to yield phytoplankton chl:C ratios consistent with laboratory findings, and the quantity 0.00035 m^{-1} is a correction factor to account for the background component of b_{bp}. (i.e., b_{bp} associated with non-P constituents that do not covary with P in the water column). Consistent with this satellite-derived background value, the median of all b_{bp} measured in our profile dataset between 200 and 300 m, where chlorophyll is negligible but other particles are present, was 0.00036 m^{-1}. Equation (2) converts chlorophyll concentration to phytoplankton carbon using a "typical" chl:C ratio of 50 g g^{-1} (a representative value for laboratory cultures [e.g., *Falkowski and Owens*, 1980; *Laws and Bannister*, 1980; *Cloern et al.*, 1995]). This chlorophyll-based approach ignores all chl:C variability associated with physiological responses to changing light and nutrient conditions (further discussed below).

[7] Mixed layer depths (MLDs) were defined for each profile as the depth at which seawater density (calculated from measured C, T, and Pr) was 0.125 kg m^{-3} greater than that at the surface [*Kara et al.*, 2000]. Following *Zawada et al.* [2005], we also computed MLDs based on the vertical locations of maximum gradients in b_{bp} and [*chl*]. The latter MLD estimates are, in general, shallower than the physically-based MLDs, as they represent recent mixing rather than the longer-term mixing associated with the 0.125 kg m^{-3} density criteria [*Thomson and Fine*, 2003].

[8] Isolume depths were calculated using surface photosynthetically available radiation (PAR) values obtained from NASA SeaWiFS data and [*chl*] values obtained from the profiling float. Based on the work by *Letelier et al.* [2004], we assume 0.415 mol quanta m^{-2} day^{-1} to be the threshold isolume below which light is insufficient to support photosynthesis, with its depth given by:

$$z(0.415) = \log\left(\frac{0.415}{0.98 * \mathrm{PAR}}\right)\left(\frac{z_{eu}}{\log(0.01)}\right), \quad (3)$$

where z_{eu} is the depth at which light is 1% of its surface value and is calculated by attenuating subsurface PAR according to the algorithm of *Morel et al.* [2007, equation (10)]. The 0.98 factor accounts for transmission through the air-sea interface. The quantity in the second bracket is the reciprocal of the diffuse attenuation coefficient for PAR.

[9] Earlier analyses showed that the chlorophyll record for the profiling float had a 20-day decorrelation scale [*Boss et al.*, 2008]. Before calculating growth rates, we therefore applied a four-point temporal box-car filter (using Matlab's filtfilt) to MLD, PAR, P_b, and P_{chl} to minimize the effects of the mesoscale variance band. No subsequent smoothing was applied to these or other derived variables.

[10] Phytoplankton biomass for each vertical profile was characterized in terms of its surface and depth–integrated values. Surface values, $P^s_{i=b,chl}$ [mg m^{-3}], were defined as the median of the upper four profile measurements of each variable (max depth 15 m). Depth-integrated values, $\int P_{i=b,chl}$ [mg m^{-2}], were obtained by integrating (trapezoidal rule) from the surface down to either the mixed-layer depth (as defined by the density-difference criterion) or the threshold isolume of 0.415 mol quanta m^{-2} day^{-1} (equation (3)), whichever was deeper. The intent here was to capture the entire actively photosynthesizing phytoplankton population. Specifically, when the base of the mixed layer is located above the threshold isolume (e.g., mid-summer), sufficient light exists below the mixed layer to support net growth, so integration is extended to the isolume depth to encompass the full active phytoplankton population. In contrast, when the base of the mixed layer is deeper than the threshold isolume, vertical mixing ensures that the entire population within the mixed layer periodically passes through the upper sunlit photic zone and thus can exhibit net photosynthesis and growth (note that mixed layer transit times are typically on the order of hours [e.g., *Denman and Gargett*, 1983]). Under these conditions therefore (e.g., fall through spring), the active biomass extends from the surface to the base of the mixed layer. This 'conditional' approach is self-consistent because, throughout our entire record, near-surface mixing was never deep enough to cause the average light level of mixed layer phytoplankton to fall below the 0.415Ei m^{-2} day^{-1} criterion. For example, observed MLDs on Dec. 21st (shortest day of the year) ranged from 80 to 100 m, while mixing to 230 m would have been necessary to reduce the average mixed layer light level to 0.415Ei m^{-2} day^{-1} (even deeper for clearer water). In addition, our 0.415Ei m^{-2} day^{-1} threshold likely represents an upper limit, as it was derived from measurements in tropical waters of the central Pacific Ocean and will not reflect other physiological states or taxonomic

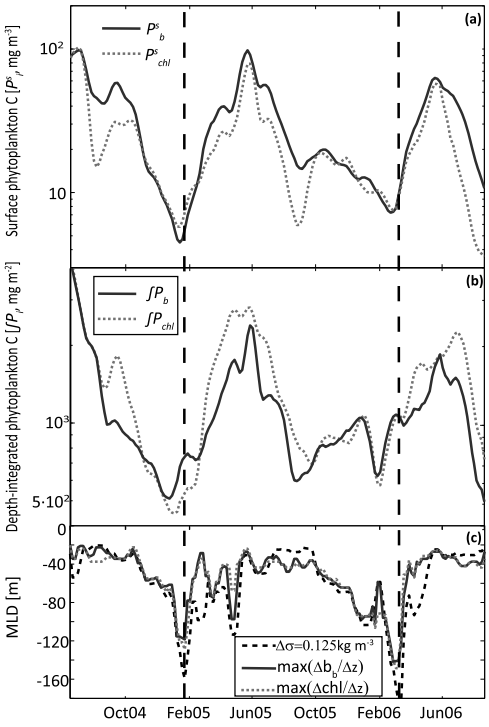

Figure 2. (a) Surface phytoplankton carbon, $P^s_{i=b,chl}$, (b) depth integrated phytoplankton carbon, $\int P_{i=b,chl}$, and (c) mixed layer depths. Vertical dashed black lines mark the times of deepest MLD during each winter season. Depth integration was performed from the surface to either the MLD or the 0.415 Ei m^2 day^{-1} isolume, whichever was greatest.

differences. For example, *Geider et al.* [1986] reported positive net growth in the temperate diatom, *Pheodactylum tricornutum*, at light levels as low as 0.11Ei m^{-2} day^{-1}. Even lower threshold irradiances are likely in phytoplankton species adapted to the low winter light levels and cold-temperatures of the subarctic Atlantic [*Smetacek and Passow*, 1990].

[11] Phytoplankton net biomass growth rates ($r_{i=b,chl}$) were calculated between observational time-points using centered-differences as follows:

$$r_{i=b,chl}(t+\Delta t/2) \equiv \begin{cases} \dfrac{1}{\overline{P}_i}\dfrac{d\overline{P}_i}{dt} \approx \dfrac{2}{\Delta t}\dfrac{\left(\overline{P}_i(t+\Delta t)-\overline{P}_i(t)\right)}{\left(\overline{P}_i(t+\Delta t)+\overline{P}_i(t)\right)} & \text{if } \dfrac{d\text{MLD}}{dt} < 0 \;\&\; MLD > z(0.415) \\ \dfrac{1}{\int P_i}\dfrac{d\int P_i}{dt} \approx \dfrac{2}{\Delta t}\dfrac{\left(\int P_i(t+\Delta t)-\int P_i(t)\right)}{\left(\int P_i(t+\Delta t)+\int P_i(t)\right)} & \text{all other cases} \end{cases} \quad (4)$$

with Δt = 5 days and $\overline{P}_i$ denoting the MLD averaged phytoplankton biomass. Note that these net biomass growth rates are independent of the multiplicative constants in equations (1) and (2) and in the instrument calibration, as they are cancelled in the derivation of the rate equation. The net growth-rate (surface versus depth-integrated value) was defined so as to include exactly that portion of the phytoplankton population exposed to light adequate to support photosynthesis. Therefore, depth-integrated carbon, $\int P_{i=b,chl}$, was used for calculation of growth rate except during periods when a mixed layer deeper than z(0.415) was shoaling (i.e., dMLD/dt < 0). Under this condition, we did not want to include in the growth rate calculations that portion of the population which is cut-off from the region where they can photosynthesize ($MLD > z(0.415)$). In that case, we used the time-rate-of-change of the ML averaged biomass, $\overline{P}_{i=b,chl}$.

[12] An illustrative example may help clarify the need for switching algorithms when the MLD is shoaling but is still deeper than Z_{eu}. Assume an initial case where the ML is 100 m and phytoplankton biomass is 0.1 mg C m^{-3}. During the next measurement, we find that the ML is 50 m deep (still deeper than z_eu) but the phytoplankton concentration has increased to 0.2 mg m^{-3}. Clearly, the phytoplankton population maintained within the mixed layer has increased in concentration, while those trapped below the mixed layer have all been lost. However, if we compute growth rate over this time interval using depth integrated biomass, we obtain $r = \ln(10 \text{ mg C m}^{-2}/10 \text{ mg C m}^{-2})/(t_1 - t_0) = 0$ divisions d^{-1}. Thus, the depth integrated calculation yields a growth rate of zero, while it is obvious that phytoplankton in the mixed layer have doubled in concentration between the successive profiles. If instead we use the change in phytoplankton concentration (i.e., m^{-3}) between the two observations (i.e., $r = \ln(0.2 \text{ mg C m}^{-3}/0.1 \text{ mg C m}^{-3})/(t_1 - t_0)$), we retrieve the correct net biomass growth rate of the growing population.

[13] One of the important developments of this study over the satellite-based study of *Behrenfeld* [2010] is that the *in situ* float data allow us to account for subsurface dynamics not visible from space, such as the entrainment of deep phytoplankton during periods of mixed layer deepening.

[14] To assess uncertainties in observed trends, we varied the ML depth criterion, the euphotic depth criterion, and the relationships between measured optical variables and estimated biomass (not shown). Some differences in net growth-rate magnitudes were observed, but the temporal patterns were found to be robust. Calculations of standard-errors in monthly climatologies of growth rates (more than ten realizations of growth rates per month) demonstrated that median net population growth rates in January and February were significantly greater than zero.

3. Results

[15] Over the two-year period of North Atlantic observations, strong annual cycles in surface- and depth-integrated phytoplankton biomass were observed for both the scattering-based (P_b) and chlorophyll-based (P_{chl}) carbon estimates (Figure 2). Values were high when observations commenced in June 2004, then dropped to a wintertime low. In mid-winter, a transition from declining biomass to a growing population was seen, culminating in peak biomass levels by late spring. A similar mid-winter transition was also seen the following year. This initiation of mid-winter biomass accumulation occurred earlier for $\int P_i$ than for P^s_i. In Figure 2, P_b and P_{chl} are plotted on log-transformed y-axes so as to provide a first-order visual sense of biomass

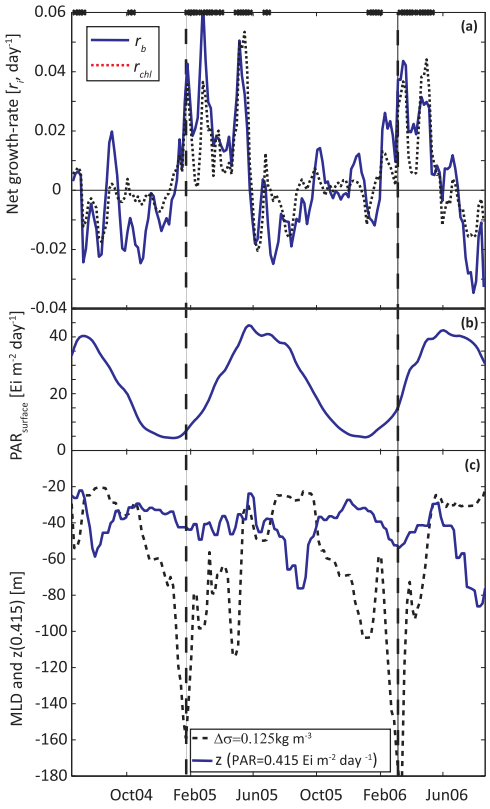

Figure 3. (a) Phytoplankton net carbon accumulation (growth) rate, $r_{i=b,chl}$, (b) SeaWiFS surface PAR, and (c) mixed layer depth and 0.415 Ei m^2 day^{-1} isolume depth. The symbols on the top edge of the top panel denote times when the growth-rate algorithm (equation (4)) is based on mixed-layer averaged carbon values rather than depth-integrated values (see text). Dashed black lines mark the times of deepest MLD. The standard-error-of-the-mean for monthly-averaged growth-rates are smaller than 0.005 d^{-1}.

growth rates. The slope of biomass versus time of such a plot is proportional to exponential growth rate, so periods of constant positive (negative) slope indicate periods of constant biomass growth (loss) rates.

[16] Differences in the temporal evolution of P_b and P_{chl} (Figure 2) are not surprising because the scalar used to convert [*chl*] to P_{chl} (equation (1)) ignores changes in cellular pigmentation levels. The basis for the observed second-order differences is revealed through changes in the P_b:[*chl*] ratio, which varied with light level in a manner consistent with photoacclimation (Figure S1 of the auxiliary material).[1] Under low-PAR conditions, this ratio decreased as light-harvesting chlorophyll was ramped up relative to phytoplankton carbon. Some fraction of the initial mid-winter population growth seen in P_{chl} is thus likely due to an increase in chlorophyll per cell rather than an increase in population numbers.

[17] Transition from negative to positive net biomass accumulation occurred during mid-winter of both years, coincident with or before the time of maximum mixed layer depth (Figures 2 and 3). Thus, initiation of North Atlantic 'blooming', sensu *Sverdrup* [1953], coincided with minimal or decreasing light levels, which would dictate low photosynthetic and specific growth rates. This finding is robust to whether biomass is assessed from the backscattering coefficient or chlorophyll (Figure 3). In addition, these *in situ*–derived growth rates are consistent with satellite-derived values [*Behrenfeld*, 2010] and, over the full bloom period, indicate rather low typical net population growth-rates of <0.05 d^{-1} (i.e., slower than population doubling every two weeks). Note that differences in the evolution of surface and depth-integrated carbon estimates during the winter (Figure 2) are mostly due to dilution of the phytoplankton population by mixed layer deepening, an effect that has been explicitly accounted for in the biomass growth rates shown in Figure 3a.

4. Discussion and Conclusion

[18] The notion of a phytoplankton bloom is associated with high biomass standing stocks [*Miller*, 2004; *Mann and Lazier*, 2006]. Consequently, studies of spring blooms often base their criteria for initiation on the achievement of some specific relative quantity of biomass, such as exceeding the annual median value by a given percentage [e.g., *Follows and Dutkiewicz*, 2002; *Siegel et al.*, 2002; *Hanson et al.*, 2009]. In contrast and in keeping with the early work [*Sverdrup*, 1953], we associate bloom initiation with the time when the phytoplankton population net growth rate becomes positive ($r_i > 0$). In doing so, we find that bloom initiation occurs prior to significant mixed layer shoaling (i.e., stratification) and PAR increase. In other words, the annual cycles of net phytoplankton biomass growth rates reported here from two years of *in situ* measurements in the North Atlantic differ from the classical view (Sverdrup's Critical Depth hypothesis) that bloom initiation *requires* springtime mixed layer shoaling beyond a critical depth.

[19] We observe significant biomass accumulation rates (comparable to springtime values) at times when phytoplankton specific growth rates would be expected to be at their lowest (i.e., when temperatures are coldest, incident light is lowest, and mixed layer depths are deepest; Figure 3 – for temperature data see *Boss et al.* [2008, Figure 7]). This finding implies that mixed layer light conditions, even during winter, did not reach levels sufficiently low to prohibit positive biomass growth rates (at higher latitudes, however, phytoplankton growth can be arrested by the complete darkness of polar night.). It is important to recognize that, while 'blooming' initiation may occur in mid-winter, peaks in phytoplankton productivity, CO_2 uptake, and carbon export remain springtime events, as these latter properties are products of phytoplankton biomass *and* specific growth rates (i.e., productivity ≡ biomass × specific growth rate).

[20] The annual cycles of phytoplankton biomass reported here de-emphasize the role of light-driven increases in phytoplankton specific growth rates for determining 'blooming' initiation and suggest a much greater role for the balance between phytoplankton growth and losses. Our findings are thus consistent with recent remote sensing observations of North Atlantic upper ocean bloom dynamics and the proposed dilution–recoupling hypothesis of *Behrenfeld* [2010]. In this scenario, mixed layer deepening decouples grazers from phytoplankton, resulting in a

[1] Auxiliary materials are available in the HTML. doi:10.1029/2010GL044174.

decrease in loss rates coincident with a wintertime decrease in specific growth rates. If grazing pressure is sufficiently diminished, then net population growth can still be positive and accumulation can occur—as was observed in our *in situ* data. When the water restratifies in the spring, under conditions of increasing insolation and decreasing winds, phytoplankton specific growth rates increase, but so do loss rates as predators are recoupled to their prey. Thus, seasonal changes in predator–prey relationships could play a central role in shaping the temporal patterns in phytoplankton biomass, adding to the environmental factors (e.g., light, nutrients, stratification, and temperature) that govern phytoplankton specific growth rates as previously suggested, for example, by *Evans and Parslow* [1985].

[21] **Acknowledgments.** This work has been supported by NASA's Ocean Biology and Biogeochemistry Program. The success of the optical profiling float is largely due to the diligent work of D. Swift. This manuscript has benefited from comments by P. Strutton and two anonymous reviewers.

References

Banse, K. (1994), Grazing and zooplankton production as key controls of phytoplankton production in the open ocean, *Oceanography*, *7*, 13–20.

Behrenfeld, M. J. (2010), Abandoning Sverdrup's critical depth hypothesis, *Ecology*, *91*, 977–989, doi:10.1890/09-1207.1.

Behrenfeld, M. J., E. Boss, D. A. Siegel, and D. M. Shea (2005), Carbon-based ocean productivity and phytoplankton physiology from space, *Global Biogeochem. Cycles*, *19*, GB1006, doi:10.1029/2004GB002299.

Boss, E., D. Swift, L. Taylor, P. Brickley, R. Zaneveld, S. Riser, M. J. Perry, and P. G. Strutton (2008), Observations of pigment and particle distributions in the western North Atlantic from an autonomous float and ocean color satellite, *Limnol. Oceanogr.*, *53*, 2112–2122.

Cloern, J. E., C. Grenz, and L. Vidergar-Lucas (1995), An empirical model of the phytoplankton chlorophyll/carbon ratio—The conversion factor between productivity and growth rate, *Limnol. Oceanogr.*, *40*, 1313–1321, doi:10.4319/lo.1995.40.7.1313.

Denman, K., and A. Gargett (1983), Time and space scales of vertical mixing and advection of phytoplankton in the upper ocean, *Limnol. Oceanogr.*, *28*, 801–815, doi:10.4319/lo.1983.28.5.0801.

Evans, G. T., and J. S. Parslow (1985), A model of annual plankton cycles, *Biol. Oceanogr.*, *3*, 327–347.

Falkowski, P. G., and T. G. Owens (1980), Light-shade adaptation, *Plant Physiol.*, *66*, 592–595, doi:10.1104/pp.66.4.592.

Follows, M., and S. Dutkiewicz (2002), Meteorological modulation of the North Atlantic spring bloom, *Deep Sea Res., Part II*, *49*, 321–344.

Geider, R. J., B. A. Osborne, and J. A. Raven (1986), Growth, photosynthesis and maintenance metabolic cost in the diatom Phaeodactylum tricornutum at very low light levels, *J. Phycol.*, *22*, 39–48, doi:10.1111/j.1529-8817.1986.tb02513.x.

Henson, S. A., J. P. Dunne, and J. L. Sarmiento (2009), Decadal variability in North Atlantic phytoplankton blooms, *J. Geophys. Res.*, *114*, C04013, doi:10.1029/2008JC005139.

Kara, A. B., P. A. Rochford, and H. E. Hurlburt (2000), Mixed layer depth variability and barrier layer formation over the North Pacific Ocean, *J. Geophys. Res.*, *105*, 16,783–16,801, doi:10.1029/2000JC900071.

Laws, E. A., and T. T. Bannister (1980), Nutrient- and light-limited growth of *Thalassiosira fluviatilis* in continuous culture, with implications for phytoplankton growth in the ocean, *Limnol. Oceanogr.*, *25*, 457–473, doi:10.4319/lo.1980.25.3.0457.

Letelier, R. M., D. M. Karl, M. R. Abbott, and R. R. Bidigare (2004), Light driven seasonal patterns of chlorophyll and nitrate in the lower euphotic zone of the North Pacific Subtropical Gyre, *Limnol. Oceanogr.*, *49*, 508–519, doi:10.4319/lo.2004.49.2.0508.

Mann, K. H., and J. R. N. Lazier (2006), *Dynamics of Marine Ecosystems. Biological-Physical Interactions in the Oceans*, Blackwell, Boston, Mass.

Miller, C. B. (2004), *Biological Oceanography*, Blackwell, Boston, Mass.

Morel, A., Y. Huot, B. Gentili, P. J. Werdell, S. B. Hooker, and B. A. Franz (2007), Examining the consistency of products derived from various ocean color sensors in open ocean (case 1) waters in the perspective of a multi-sensor approach, *Remote Sens. Environ.*, *111*, 69–88, doi:10.1016/j.rse.2007.03.012.

Siegel, D. A., S. C. Doney, and J. A. Yoder (2002), The North Atlantic spring bloom and Sverdrup's critical depth hypothesis, *Science*, *296*, 730–733, doi:10.1126/science.1069174.

Smetacek, V., and U. Passow (1990), Spring bloom initiation and Sverdrup's critical-depth model, *Limnol. Oceanogr.*, *35*, 228–234, doi:10.4319/lo.1990.35.1.0228.

Sverdrup, H. U. (1953), On conditions for the vernal blooming of phytoplankton, *ICES J. Mar. Sci.*, *18*, 287–295, doi:10.1093/icesjms/18.3.287.

Thomson, R. E., and I. V. Fine (2003), Estimating mixed layer depth from oceanic profile data, *J. Atmos. Oceanic Technol.*, *20*, 319–329, doi:10.1175/1520-0426(2003)020<0319:EMLDFO>2.0.CO;2.

Zawada, D. G., J. R. V. Zaneveld, E. Boss, W. D. Gardner, M. J. Richardson, and A. V. Mishonov (2005), A comparison of hydrographically and optically derived mixed layer depths, *J. Geophys. Res.*, *110*, C11001, doi:10.1029/2004JC002417.

M. Behrenfeld, Department of Botany and Plant Pathology, Oregon State University, Cordley Hall 2082, Corvallis, OR 97331, USA.

E. Boss, School of Marine Sciences, University of Maine, 5706 Aubert Hall, Orono, ME 04469, USA. (emmanuel.boss@maine.edu)